

Responses to Reviewer's questions

Our grateful thanks to the Reviewer for valuable comments and thorough analysis of the work, which we believe has really enhanced the manuscript. Our responses are presented below. The deep language correction of the manuscript was also performed by native.

Suggestions for revision or reasons for rejection (will be published if the paper is accepted for final publication)

This manuscript discusses the application of artificial neural networking (ANN) techniques to the previously developed BARDet fluorescence detection system, as well as the potential application to aerosol characterization. In this study, the authors aerosolized 48 different fluorescent aerosols and attempted to model a system of artificial neural networks into a decision tree to appreciably categorize the measured particles. The resulting system was 22 sets of ANNs to totally classify the overall data set over multiple iterations. Real-time and inexpensive bioaerosol classification is an extremely important step to understanding the overall effects bioaerosols have on the environment and climate, and so a paper addressing such could be of great interest AMT community. However, there are some issues here that need to be addressed prior to considering acceptance.

Major

1. Leaving out non-fluorescent particles may be a bigger challenge to successfully implementing the ANNs than the authors suggest, considering that the majority of atmospheric aerosols are largely "non-fluorescent." There's no justification of this further in the text of this manuscript other than the statement in line 195 regarding application of a threshold. Separating a host of fluorescence particle types is one thing, but an atmospheric sample is going to contain an extreme minority of fluorescent particles. A recent study (Savage et al., 2018) utilized HAC techniques to attempt to classify similar types of particles, though the high-thresholding needed to get rid of the majority of the "non-fluorescent" particles ultimately confounded the clustering algorithm due to an appreciable number of "fluorescent" particles being removed as well. If this paper is going to move forward, this needs to be addressed as a limitation of the study. For example, I suggest discussing that nonfluorescent particles being absent is a limitation for usage in ambient studies, though future work could include them in attempts to mimic ambient conditions.

- We agree with Reviewer and we are aware that non-fluorescent particles are dominant in the atmosphere, therefore, their characterization is very important and should not be neglected. However, there is no single technique capable of fully characterizing the entire population of particles in the ambient air. The UV-LIF detectors are intended mainly for detection of biological particles basing on their fluorescence properties. Alternatively size or/and shape of the particles can be measured. There is still no information concerning the bio/chemical composition of measured particles. In our opinion the ANNs alone does not limit "non-fluorescent" particle analysis. They can analyze any type of data and the final result depends on

the number, quality and physicochemical parameters which will be used as an input data.

- Regarding the line 195 (currently 122) we justified the types of aerosols tested not the algorithm of data preprocessing. Savage et al. (2018) used intensity thresholds to “extract” stronger signals from those of lower ones. In our experiments all (low and high) fluorescence signals has been considered, but the particles which are non-fluorescent by nature like gypsum, soot, Syloid etc. has not been investigated.
- In the Introduction section in lines 58-60 we added as follows: “ Besides advantages such as reagentless and real time particle characterization, the laser based methods do not provide information on the chemical composition of aerosol.. “
- In the last sentence of the Summary we added as follows: “... which will be most challenging due to the presence of unknown fluorescent and non-fluorescent particles .”
- Of course in real atmospheric studies, that are already planned, the non-fluorescent particles will be considered.

2. The section describing the ANN generation and decision tree processing needs to clarify that this process isn't replicable in terms of the exact factors used for ANN generation, and that the ANN decision-tree generation results may be different with subsequent trials. A response to reviewer 3 from the first submission discusses this in length (ie how the weights/start factors are randomly chosen). I understand this was a real-time attempt as classification, but specific factors being non-replicable as well as having no secondary decision-tree development trials shown, and utilizing a new type of instrument only available to these researchers, can greatly limit possible impacts of this manuscript. This is only compounded by the first point (No non-fluorescent particles probed) in that what was done here may not be applicable to ambient data sets.

- In the section 4.3 in line 371 the following sentence was inserted: “ The process of creating them is not replicable in terms of the exact factors used for ANN generation. However, this is not essential, because the decision tree is based on ANN results (classification ability), which should be possibly the highest. Therefore, the final result will be the same.”
- We agree with the Reviewer's opinion that instrument and developed software has limited usage by other researchers. On the other hand it is prototype that is still developed, but it potentially may be available commercially in a few years. It is worth to note that for example WIBS family instruments has not been available to other researchers. They are still unavailable for us due to the price. From the practical point of view, it is essentially important to share our experience concerning the new approach to use ANNs to real-time aerosol classification. In the next step we

are going to undertake a challenge of real atmospheric data analysis to test the real applicability of the system.

3. The sizes of individual particle types, as well as asymmetry factor, are listed in table 2 for each particle type. It's not clear from the text that these parameters are being used in the ANNs in any way, and in fact the opposite seems to be the case. In terms of the sizes of particles, there are three sub-points:

- The particle sizes and asymmetry factors were proposed by other Reviewer, who suggested the full characterization of the aerosols. Actually those data were not used for aerosol analysis. For ANN analysis only the fluorescence data was used. Numerous trials has shown that best classification was achieved using fluorescence data only.

a. Some of these pollen particles are seen around 85 microns (*A. alba*), and relatively small particles around 2 microns (Riboflavin) are also being measured. Other commercial UV-LIF instrumentation have issues with detecting simultaneously small and large particles without having limit of detection or saturation issues respectively. The 2016 paper shows some information on size dependence, but only goes up to 8 microns. A statement about the dynamic range of the instrumentation would be helpful here.

- We are aware that commercial devices has been tested in more detail than BARDet which was developed recently and still it is modified and improved. The instrument has been calibrated for particle sizing up to 8 microns because of limited availability of standards in the project. The further research is beyond the scope of the recent grant.
- Regarding the simultaneous detection of low and strong signals we applied entirely new approach. The commercial UV-LIF detectors acquire integrated fluorescence signals in 1-3 fluorescence bands that is likely to produce saturated signals in single window PMT. In the BARDet the fluorescence signal is "distributed" among 18 channels grouped in 7 spectral bands. It assures simultaneously high S/N ratio due to summing low signals as well as prevents the signal saturation by narrow band entering the single PMT channel. It is clearly presented by non-saturated fluorescence characteristics of highly fluorescent riboflavin or FM7 microspheres (Fig. 2).
- In lines 104-106 we added sentence as follows: " Such a solution extends the dynamic range of measured spectra and, assures a high S/N ratio, and also reduces the possibility of signal saturation. ."

b. The average and standard deviation of size is mentioned in this chart, though with no units attached. This needs to be addressed on the table. With the FM7 measurements listed, it appears to be in microns. It is unlikely that the authors would be measuring intact pollen grains with such aggressive sampling methods (intense vortexing/vibration). Aerosolization of pollen has been seen to rupture pollen in previous studies (Hernandez et al., 2016; Savage et al., 2017) as well, let alone aggressive vortexing/vibration. The low uncertainty on

the measurements (e.g. 44.8 + 2.01 for *S. cereale* pollen) also points to intact pollen being measured.

- The missing data concerning particle size units in Table 2 has been completed with “um”.
- The data concerning particle sizes in Table 2 are acquired after aerosolization of the samples and collecting them on glass slides. The method we applied was developed especially for non-disruptive aerosol generation. In the experiments gentle vortexing and low air flows has been applied. We agree with Reviewer that pollen fragmentation occurs. However, in the nature pollen grains are resistant to harsh environmental conditions. We checked again the microscopic image and in fact *S. cereale* grains were intact at least at chosen frame. We do not insist that some of particles were not fragmented. In some cases it was difficult to find representative frame due to low concentration of particles. Moreover, we have noticed that the pollen rupture can occur also inside of the device’s nozzle, therefore we think that our aerosol generation method is not the main reason of pollen rupture.

c. Why was only the normalized spectral shape used in the ANN decision making? In a particularly bad example buckwheat flour and cellulose were effectively unable to be classified against one another, though these two particles types showed very different average size and asymmetry factors.

- As it was mentioned earlier there is no single method allowing complete aerosol analysis including size, shape, fluorescence, biological or chemical composition. The advantage of LIF based devices is real-time and no sample preparation analysis. Various naturally occurring biological particles of different origin will fluoresce in similar pattern therefore they will be difficult to distinguish. The numerous approaches has been made concerning input data normalization and selecting which input data should be considered (fluorescence only, fluorescence + scattering). The best results were achieved for fluorescence which is always unchanged in character, while the scattering strongly depends on particle position in interrogation point. The data normalization is essential for proper data calculation and comparison.

4. The paragraph beginning on line 53, describing fluorescent particles and their detection/characterization, seems to be missing several key papers, as well as cites a paper (Hernandez et al., 2016) that is irrelevant to the discussion there. Pan et al., 2007; Crawford et al., 2015; Ruske et al. 2017, 2018; Savage et al., 2017 and 2018 are all examples of recent work that support recent work in the area discussed in the referenced sentence.

- We agree with Reviewer that one of the paper is not a best choice at this point. According to the Rewiever’s suggestion the article by Crawford at al. 2015 and Savage et al 2017 has been added.

5. There needs to be mention of the absence of nonfluorescent particles in the abstract, and that further work would need to probe this.

- In the abstract we added last paragraph as follows: “ In the future, it is planned that performance of the system may be determined under real environmental conditions, involving characterization of fluorescent and non-fluorescent particles .”

6. Usage of the word “real-time” in the abstract is misleading, because while the instrument does measure in real time the data was collected separately (per aerosol type). The time-component for this study is irrelevant in this case.

- It is true that database collection was separate process. However, as soon as the aerosols library was implemented to the algorithm the next measurements automatically generated immediate aerosol recognition. The term “real-time” relates to measurement of aerosol “fluorescence fingerprints” as well as the data analysis. In this point we refer to supplementary material attached to our article Kaliszewski et al., 2016 which clearly visualizes real-time PCA. The ANN are not so easy to visualize that’s why we show final results.

Minor (or Technical) Points

1. Raw number of particles per aerosolized particle type is not listed here, and instead a raw number total (114779) for the entire data set is listed, with an average spectra per total listed (~2400). This needs to be addressed, as the statement of 2400 average could be true, though it could also be misleading.

- Actually the average number of spectra can be misleading. In the table statistical data of measurements are presented.

all particles for 48 substances	114751
min	1548
max	3609
average	2391
standard deviation	437

- The sentence in the line 216 has been changed to following: “ Finally, a total of 114,779 spectral characteristics of 48 aerosols was gathered, which gives on average 2391 (standard deviation 437) fluorescence characteristics per substance .”

2. Take out the word “impressive” on line 30 (before effectiveness)

- The sentence actually sounds as follows: “As a result, a very high accuracy of aerosol classification in real-time was achieved.”

3. Line 119: Leaf scraps should be “leaf litter”

- After reconsideration and literature analysis we assume that “Plant debris” is most suitable term.

4. Naming of things in Table 2 not consistent (e.g. pollen types - some scientific name, some common name), nor are the abbreviations (e.g. Ambio vs FM7 vs PF) which is distracting to the overall data.

- The pollen types in Table 2 has been updated with scientific and common names. The abbreviations were changed as follows: Ambio to AMB, Cin to CIN, Rib to RIB, FM7 to FM. All those abbreviations in the text and in the figures has been updated. The abbreviations Trp and Phe are standard in internationally recognized for aminoacids and remained unchanged.

5. Graph styles are not consistent (Figure 7 and 8 ROC graphs have different tick numbering, as well as background line densities) which is distracting to the overall presentation of the data.

- The tick numbering has been unified.

6. The text size on certain figures (8 and 9) need to be increased, as well as the ROC graphs are low-resolution compared to the confusion matrices listed.

- The text sizes in graphs has been increased from 14 to 18 points. All the figures are in 300 dpi resolution.

7. Line 72: "The simple statistics" isn't the correct syntax. Maybe "simpler statistical analysis"

- The sentence was corrected.

8. Line 119: This line makes no sense currently, and needs reworked.

- The sentence was corrected as follows: "Due to technical limitations, samples other than pharmaceutical could not be aerosolized in this study".

9. Line 194: "The non-fluorescent particles were not a subject of the research since they can be automatically discarded as non-biological applying given fluorescence threshold." This line needs taken out, because it is fundamentally wrong. As addressed above, the non-fluorescent removal via higher thresholding isn't sufficient reasoning to claim they're going to efficiently be removed because this gets rid of a large overall number of particles (Savage et al., 2017, Savage et al., 2018) and can confound HAC clustering, at the very least. This needs to be mentioned, but as a limitation overall of the scope of this paper.

- In the Major suggestions section p. 1of the response to the Reviewer we answered to this comment. The paper bt Savage was cited.

10. Fluoromax Microspheres are cited as the material used for the FM7, though it doesn't cite the particular fluorescent type (usually listed as a color) used.

- We agree with the Reviewer that the information about the colour of FM7 microspheres is missing. In Table 2 we added information that green fluorescent microspheres were used.

11. Figure 2's usage of 50 spectra-per-type is more confusing than not to how the input data is used for the ANN training. I assume if the reported 2400 spectra had been visualized it would be much busier, but this gives the impression that the training data only used 50 spectra for each aerosol type, which may or may not be the case.

- Presentation of some spectra representing input data was suggested by other Reviewer. We showed 50 example spectra per one graph since it seems to be optimal for clear presentation. Visualization of 2400 spectra does not make a sense and is practically unachievable with our graphical program module. In the figure description we changed: "Normalized 50 subsequent fluorescence characteristics..." to "Example, normalized 50 subsequent fluorescence characteristics...". In line 200 we inserted the sentence: "From the recorded data 80% was used as a training data set and 20% as test data set." We hope that modified description will be less confusing.

12. Line 16: The term "air contamination" is not usually associated with biological particles, unless there is a specific source of contamination like a waste facility or a mold outbreak.

- The term "air contamination" has been changed to "air pollution".

13. Figure 2 significant figures listed are not uniform for all Size and Asymmetry Factor measurements.

- We are not sure how to answer to the Referee's comment referring to the Size/Assymetry Factor. Figure 2 presents example fluorescence characteristics (not Size/Assymetry Factor) of three different substances.

Improved real-time bio-aerosol classification using Artificial Neural Networks

Maciej Leśkiewicz¹, *Miron Kaliszewski², Maksymilian Włodarski², Jarosław Młyńczak², Zygmunt Mierczyk², Krzysztof Kopczyński².

1. PCO S.A. ul. Jana Nowaka-Jeziorańskiego 28, 03-982 Warsaw, Poland.
2. Institute of Optoelectronics, Military University of Technology, ul. Gen. Witolda Urbanowicza 2, 00-908 Warsaw, Poland

*Corresponding author: miron.kaliszewski@wat.edu.pl

Keywords: Bio-aerosol, Fluorescence, Real-time analysis, Artificial Neural Network, PBAP.

1. Abstract

Air [pollution](#) has had an increasingly powerful impact on the everyday life of humans. Ever more people are aware of the health problems that may result from inhaling air which contains dust, bacteria, pollens or fungi. There is a need for real-time information about ambient particulate matter. Devices currently available on the market can detect some particles in the air but cannot classify them according to health threats. Fortunately, a new type of technology is emerging as a promising solution.

Laser based bio-detectors are opening a new era in aerosol research. They are capable of characterizing a great number of individual particles in seconds by analyzing optical scattering and fluorescence characteristics. In this study we demonstrate the application of Artificial Neural Networks (ANNs) to real-time analysis of single particle fluorescence fingerprints acquired using BARDet (a Bio-AeRosol Detector). 48 different aerosols including pollens, bacteria, fungi, spores, and non-biological substances were characterized. An entirely new approach to data analysis using a decision tree comprising 22 independent neural networks was discussed. Applying confusion matrices and ROC analysis the best sets of ANNs for each group of similar aerosols was determined. As a result, [a very high accuracy](#) of aerosol classification in real-time was achieved. It was found that for some substances that have characteristic spectra almost each particle can be properly classified. Aerosols with similar spectral characteristics can be classified specific clouds with high probability. In both cases the system recognized aerosol type with no mistakes.

[In the future, it is planned that performance of the system may be determined under real environmental conditions, involving characterization of fluorescent and non-fluorescent particles.](#)

2. Introduction

Ambient air contains a variety of particles such as dust, bacteria, pollens, fungi and other particles of biological and non-biological origin (Pöhlker et al., 2013; Górny, 2004). Aerosols are involved in various atmospheric processes such as ice nuclei formation, precipitation and global climate effects (Deguillaume et al., 2008; Fröhlich-Nowoisky et al., 2016; Gabey et al., 2010; Pósfai and Buseck, 2010; Fuzzi et al., 2015). They also greatly influence human health (Davidson et al., 2005; Pope and Dockery, 2006; Michaels, 2017; Shiraiwa et al., 2012). Therefore, the characterization of ambient air is important for estimating potential health hazards and environmental impact (Mauderly and Chow, 2008; Lim et al., 2005). Standard methods of aerosol composition assessment usually include microscopic inspection or molecular analysis of filters (Miaskiewicz-Peska and Lebikowska, 2012), tape or liquid trapped particles. Nevertheless, they suffer from low time

Deleted: contamination

Deleted: an impressive

Deleted: effectiveness

Deleted: ossible

Deleted: ¶

52 resolution due to periodical and relatively long analytical procedures. They are also ineffective for the
53 detection of non-culturable microorganisms (Blais-Lecours et al., 2015; Trafny et al., 2014).

54 The detection and classification of biological particles is possible using fluorescence techniques
55 due to the presence of proteins, NADH, and some vitamins that emit light when excited with UV light
56 (Lakowicz, 2006). This feature is utilized in single particle fluorescence detectors. In the flowing air
57 each particle is characterized for size/shape using light scattering as well as fluorescence properties.
58 This approach ensures continuous measurement and immediate response. Thus the analysis process
59 can be facilitated and accelerated compared with other commonly used analytical procedures (Hill et
60 al., 1999; Choi et al., 2014; Taketani et al., 2013; Feugnet et al., 2008). [Besides advantages such as
61 reagentless and real time particle characterization, the laser based methods do not provide
62 information on the chemical composition of aerosol.](#)

63 Several studies using single particle fluorescence detectors have demonstrated that fluctuations
64 of aerosol concentration and variations in its fluorescence properties are highly dependent on the
65 season, day, time, location and place occupancy (Gabey et al., 2011; Huffman et al., 2010; Pinnick et
66 al., 2004; Bhangar et al., 2014; Fennelly et al., 2017). Each single particle passing the instrument is
67 labelled with a time stamp, scattering properties (size and/or shape) and fluorescence
68 characteristics. It is obvious that continuous single particle measurements bring a new potential and
69 quality to environmental research. However, particles of the same type and batch display slightly
70 different spectral characteristics due to variations in biochemical composition, size, age of population
71 (Agranovski et al., 2003), degradation (Hernandez et al., 2016) or stress level (Lee et al., 2010) and
72 the particle position within the instrument's interrogation point (Pan et al., 2011). [Simpler statistical
73 analyses, such as](#) data averaging and graphical spectra representation, are not sufficient. Therefore,
74 the huge amount of data and occurring spectral variations require more advanced algorithms
75 supporting automatic data classification. Various analytical methods of particle discrimination and
76 classification have been applied. It has been shown that Principal Component Analysis (PCA), Linear
77 Discriminant Analysis (LDA), Hierarchical cluster Analysis (HCA) of fluorescence spectra greatly
78 increase discrimination of particles compared with methods based on spectra averaging or
79 fluorescence threshold (Leśkiewicz et al., 2016; Kaliszewski et al., 2013; Pan et al., 2012; [Savage et al.,
80 2017; Crawford et al., 2015](#)). Artificial neural networks (ANNs) comprise an emerging analytical
81 approach that is becoming more widely and successfully applied in various life domains such as
82 chemical analysis (Borecki et al., 2008), image recognition (Antowiak and Chałasińska-Macukow,
83 2003), data mining and weather forecasting (Purnomo et al., 2017). It has been shown that ANNs can
84 be applied in bio-aerosol classification (Kohlus and Bottlinger, 1993). However, it usually requires
85 more user input compared to other analytical procedures (Ruske et al., 2017).

86 This paper focuses on the application of ANNs for real time discrimination of bio-aerosols based
87 on single particle fluorescence characteristics. We demonstrate a new approach to data analysis
88 using ANNs which allows automation of data preparation procedures and minimum user
89 involvement.

91 3. Materials and methods

92 3.1. Experiment

93 3.1.1. BioAeRosol Detector (BARDet)

94 Detailed information concerning the construction and parameters of the instrument used for
95 the experiments was presented in our previous work (Kaliszewski et al., 2016). In general, the
96 ambient air is continuously drawn through the nozzle. It is focused with a sheath flow of filtered air.

Deleted: Savage et al., 2017; Crawford et al., 2015)

Deleted: (Hernandez et al., 2016)

99 Particles in the focused air pass through the BARDet's chamber where they are interrogated by a
100 16mW CW laser beam generated by a diode laser operating at 375 nm wavelength (CUBE, Coherent).
101 The backward and forward scattered signals are detected with two PMTs (H6780, Hamamatsu)
102 mounted at the 35° and 145° angles to the laser beam axis.

103 The fluorescence of particles is measured at a 90° angle to the laser beam with 32 channel PMT
104 (A10766, Hamamatsu). The longpass filter with cutting edge at 400 nm (Edmund Optics) separates
105 the fluorescence signal from scattered light. The multichannel PMT measures fluorescence in 18
106 active channels in a range of 415.4-643.5 nm. The channels are grouped in 7 bands. [Such a solution](#)
107 [extends the dynamic range of measured spectra and, assures a high S/N ratio, and also reduces the](#)
108 [possibility of signal saturation.](#) The remaining channels are not used. The band configuration is
109 presented in Table 1.

Deleted: .

110
111 Table 1. Configuration of bands in the multichannel PMT.

BARDet's Fluorescence Bands	Bandwidth [nm]
B1	415.4 – 429.3
B2	443.1 – 456.8
B3	470.5 – 484.2
B4	497.8 – 524.9
B5	538.3 – 565.0
B6	578.3 – 604.6
B7	617.6 – 643.5

113
114 **3.1.2. Aerosols**

115 For the tests, dry powders of harmless substances were used since they did not need a
116 specialized aerosol protection chamber. In order to achieve a reliable aerosol classification, the ANNs
117 need to be trained possibly using a large number of measurement data. Therefore, various particle
118 types, that can be easily aerosolized, were tested. Samples such as pollens, fungi, bacteria, spores
119 and [plant debris](#) naturally occur in the atmosphere. Biofluorophores such as riboflavin, cellulose,
120 amino acids and proteins were also characterized since they are present in biological materials. The
121 group of bacterial growth media was investigated due to their powerful influence on bacteria
122 fluorescence especially if they are not sufficiently washed. This can occur in the case of intentionally
123 released bacterial aerosols. Due to technical limitations, samples other than pharmaceutical could
124 [not](#) be aerosolized in this study. The aerosols of flours, and fluorescent non-biological substances
125 such as paper dust, AC fine Test Dust and talc were analyzed since they can occur especially in indoor
126 and public places. Non-fluorescent particles were not a subject of the research since they can be
127 automatically discarded as non-biologically applying given fluorescence thresholds.

Deleted: leaf scraps

128 The samples used for this study are listed in Table 2. To perform numerous experiments,
129 disposable vials were used, one for each aerosol sample. This prevented cross contamination
130 between measured samples. The aerosols were generated from modified 50 ml Falcon tubes placed

133 on the vortex. The vials in the lower part contained two connectors for silicon tubes. Vortexed
 134 particles were entrained and formed an aerosol cloud inside the Falcon tube. The aerosolized
 135 particles were aspirated from the vial to BARDet's aerosol inlet. Each tube contained about 50 mg of
 136 the dry powder sample. During aerosol generation, filtered air was supplied into the vial to
 137 compensate for the BARDet's flow. The concentration of the aerosols was adjusted with vibration
 138 frequency of the vortex. The measurement started after the aerosol reached a homogeneous
 139 concentration. The experimental setup is shown in Figure 1.

140

141 Table 2. List of all substances used in the experiment.

142

	Abbreviation	Name	Size [μm]	AF	Source	Group	
1	FM	Fluoromax green fluorescent 7 μm microspheres	6.25 \pm 0.91	0.92 \pm 0.02	Thermo scientific	standard 1	
2	RIB	Riboflavin	2.22 \pm 1.82	0.88 \pm 0.09	Sigma-Aldrich	standard 2	
3	BGP	<i>Cynodon dactylon</i> (Bermuda grass)	28.35 \pm 0.6	0.97 \pm 0.01	Duke Sci. Corp.	pollens	
4	CP	<i>Zea mays</i> (Corn)	78.13 \pm 1.22	0.95 \pm 0.01	Duke Sci. Corp.		
5	CA	<i>Corylus avellana</i> (Common hazel)	27.71 \pm 1.33	0.67 \pm 0.04	(*OC)		
6	LP	<i>Lycopodium</i>	30.67 \pm 1.2	0.94 \pm 0.01	Fluka		
7	PPP	<i>Poa pratensis</i> (Kentucky bluegrass)	30.62 \pm 0.87	0.94 \pm 0.01	Sigma-Aldrich		
8	RP	<i>Ambrosia</i> (Ragweed)	19.48 \pm 0.78	0.99 \pm 0.01	Duke Sci. Corp.		
9	SCP	<i>Secale cereale</i> (Rye)	44.8 \pm 2.01	0.94 \pm 0.01	Sigma-Aldrich		
10	SP	<i>Picea</i> (Spruce)	70.09 \pm 4.16	0.88 \pm 0.02	(*OC)		
11	AA	<i>Abies alba</i> (Silver fir)	84.56 \pm 12.77	0.92 \pm 0.02	(*OC)		
12	UDP	<i>Urtica dioica</i> (Common nettle)	14.99 \pm 1.26	0.9 \pm 0.05	(*OC)		
13	PSP	<i>Pinus sylvestris</i> (Scots pine)	39.29 \pm 1.44	0.93 \pm 0.02	(*OC)		
14	PNP	<i>Pinus nigra</i> (Black pine)	44.97 \pm 1.33	0.88 \pm 0.03	(*OC)		
15	LPP	<i>Lycopodium</i> (Poland)	28.66 \pm 0.6	0.95 \pm 0.01	(*OC)		
16	PMP	<i>Broussonetia papyrifera</i> (Paper mulberry)	13.57 \pm 0.88	0.94 \pm 0.04	Duke Sci. Corp.		
17	ATP	<i>Artemisia tridentata</i> (Big Sagebrush)	22.53 \pm 0.42	0.96 \pm 0.01	Sigma-Aldrich		
18	AAP	<i>Artemisia absinthium</i> (Wormwood)	18.37 \pm 1.51	0.96 \pm 0.02	Sigma-Aldrich		
19	CPP	<i>Chenopodium</i>	27.29 \pm 0.97	0.98 \pm 0.01	(*OC)		
20	BWF	Buck wheat flour	25.17 \pm 15.76	0.82 \pm 0.06	MELVIT Poland (*RS)		flours
21	PF	Potato flour	21.23 \pm 3.11	0.96 \pm 0.03	KUPIEC Poland (*RS)		

Formatted Table

Deleted: 7

Deleted: 7 μm

Deleted: Rib

Deleted: pollen

Deleted: pollen

Deleted: pollen

Deleted: pollen

Deleted: pollen

Formatted: Font: Italic

Deleted: pollen

Deleted: pollen

Deleted: pollen

Deleted: pollen

Deleted: pollen

Deleted: pollen

Deleted: pollen

Deleted: pollen

Deleted: pollen

Deleted: pollen

Deleted: pollen

Deleted: pollen

Deleted: pollen

22	RF	Rice flour	18.22±6.23	0.6±0.07	MELVIT Poland (*RS)	amino acids and proteins
23	TF	Tapioca flour	12.91±3.41	0.7±0.06	COCK BRAND (*RS)	
24	WF	Wheat flour	20.57±4.36	0.62±0.07	MELVIT Poland (*RS)	
25	Trp	Tryptophan	15.42±8.96	0.81±0.08	Sigma-Aldrich	
26	Phe	Phenylalanine	10.41±5.31	0.73±0.11	Sigma-Aldrich	
27	BSA	Bovine Serum Albumin	63.8±30.49	0.43±0.05	POCH Poland	
28	OVA	Ovalbumin	26.45±5.31	0.83±0.07	POCH Poland	
29	AMBAMB	<i>Bif. animalis</i>, <i>S. boulardii</i>, <i>S. thermophilus</i>, <i>L. casei</i>, <i>L. bulgaricus</i>	27.97±4.42	0.84±0.03	AMBIO Probiotyky, Lab. Galenowe Poland (*P)	
30	LCB	<i>Lactobacillus bulgaricus</i>	51.16±19.33	0.68±0.08	LakciBios, ASA Poland (*P)	
31	LF	<i>Bifidobacterium animalis</i> , <i>L. acidophilus</i>	32.62±8.45	0.82±0.07	Linex forte, LEK Pharmaceuticals d.d. Slovenia (*P)	
32	BA	Bacteriological Agar	49.47±10.03	0.74±0.07	Sigma-Aldrich	medium
33	BAB	Blood Agar Base	18.78±2.11	0.71±0.12	Sigma-Aldrich	
34	LB	Luria broth	15.11±6	0.67±0.07	Sigma-Aldrich	
35	NB	Nutrient broth	42.67±9.21	0.69±0.03	Sigma-Aldrich	
36	BTSTG	<i>Bacillus thuringiensis</i> spores technical grade	7.13±5.95	0.72±0.12	Agricultural	Bacterial spore with admixtures
37	SB	<i>Saccharomyces boulardii</i>	57.82±7.56	0.69±0.05	Enterol, Biocodex France (*P)	fungi with admixtures
38	SC	<i>Saccharomyces cerevisiae</i>	21.33±5.55	0.76±0.07	Dr. Oetker Germany (*RS)	
39	LS	<i>Lycoperdon</i> spores	14.52±0.62	0.92±0.02	(*OC)	fungal spores
40	JGSS	Johnsons grass smut spores	6.91±0.34	0.98±0.02	Duke Sci. Corp.	smut spore (fungal spore)
41	BGSS	Bermuda grass smut spores	6.47±0.27	0.97±0.02	Duke Sci. Corp.	
42	ACFTD	AC Fine Test Dust	3.47±2.34	0.87±0.09	Duke Sci. Corp.	other
43	NT	Nivea talc	14.33±4.71	0.77±0.09	Nivea Baby (*RS)	
44	PPD	Printer paper dust	76.37±18.89	0.43±0.11	XEROX Laserprint collected from paper shredder (*RS)	
45	PTD	Paper towel dust	73.45±25.65	0.56±0.15	Merida Poland collected from crushed towel (*RS)	
46	CIN	Cinnamon	23.97±4.39	0.78±0.05	Kamis Poland (*RS)	
47	CEL	Celulose	82.86±14.28	0.25±0.04	Sigma-Aldrich	

Deleted: Ambio

Formatted Table

Formatted Table

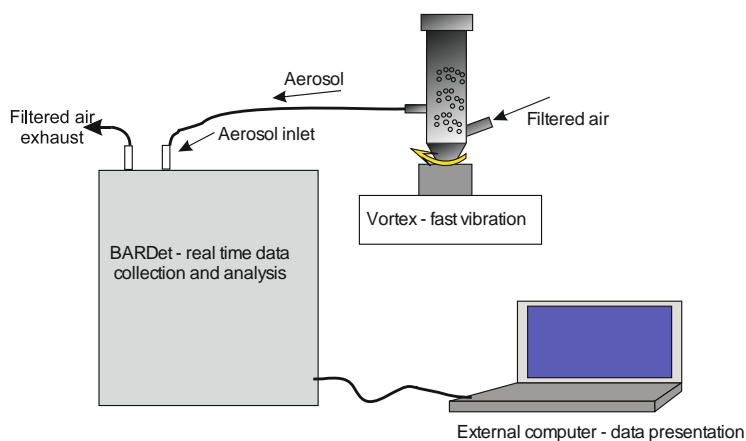
Deleted: Cin

Deleted: C

Deleted: el

48	GGL	Ground Green Leaves	18.03±4.3	0.77±0.09	Dried and ground Oak (*OC)	
----	-----	---------------------	-----------	-----------	----------------------------	--

167
 168 *OC – pollens collected from trees, flowers and grass at the region of Warsaw during vegetative
 169 seasons in 2015 and 2016.
 170 *RS – Regular shops in Warsaw where common goods are purchased.
 171 *P – Pharmacy shops in Warsaw
 172



173
 174 Figure 1. Setup of aerosol generation, data recording and analysis.

175
 176 **3.1.3. Aerosol microscopy**

177 For microscopy analysis the aerosols were generated as described above and collected by
 178 impaction on a glass microscopic slide. The visualization of the samples was performed using a Nikon
 179 Eclipse Ti-U microscope with 10x objective. The images were recorded with a 5-megapixel DS-Fi1
 180 camera. The aerosol equivalent diameters and circularity were analyzed automatically using NIS-
 181 Elements 64bit 3.22.10 software. The threshold of particle outline was corrected manually to obtain
 182 the visually best fit.

183
 184 **3.1.4. Data acquisition method and pre-processing**

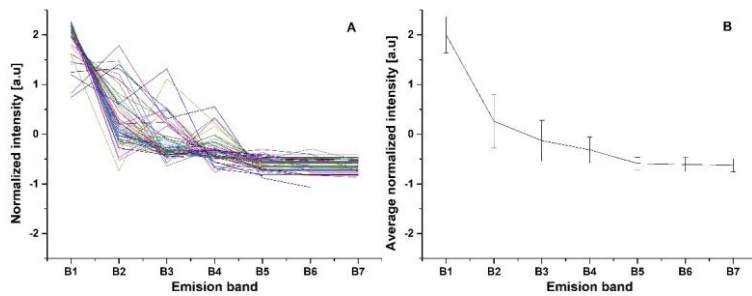
185 The fluorescence of each particle was recorded in 7 bands. This creates a time series of the
 186 signals which has to be pre-processed before further analysis. There are two steps in gathering data.
 187 The first one is performed by the internal BARDet's software which is responsible for controlling the
 188 instrument and the acquisition of raw signals. Then data is forwarded to a pre-processing module in
 189 the analysis software. Its first task is to extract valuable signals from the noise (three sigma rule).
 190 After that a normalization procedure is required. It is performed first by subtracting the average value
 191 of the signal and then normalizing it to its standard deviation. The main goal was to analyze the shape
 192 of the emission spectrum (not signal strength). An example visualization of input data is shown in
 193 Figure 2.

194 The data acquisition process started after the stabilization of the aerosol generation rate which
 195 was measured by the device. It was important not to exceed one particle per 2 ms of data integration

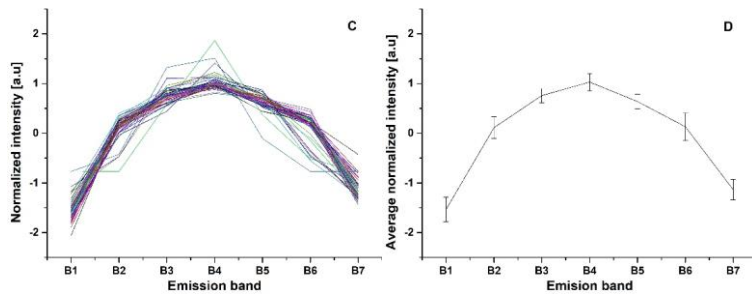
196 time in a 20 us measurement window. Finally, a total of 114,779 spectral characteristics of 48
197 aerosols was gathered, which gives on average 2391 (standard deviation 437) fluorescence
198 characteristics per substance. From the recorded data 80% was used as a training data set and 20% as
199 a test data set.

Deleted: almost 2400

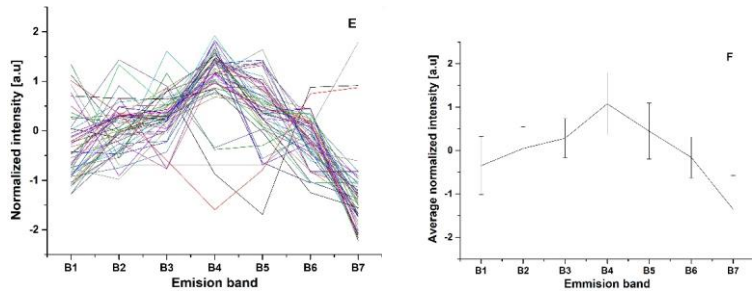
200



201



202



203

204 Figure 2. Example, normalized 50 subsequent fluorescence characteristics of NT (A), FM (C) and
205 LCB (E) and corresponding averaged normalized intensities of NT (B), FM (D) and LCB (F). Error bars
206 represent standard deviation of measurements.

207

3.2. Data analysis

208

3.2.1. ANN (Artificial Neural Network)

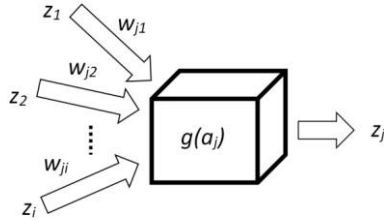
209

3.2.1.1. Basics

210

211

213 There are many types of Artificial Neural Networks (ANNs), but in this paper only the
 214 backpropagation algorithm is demonstrated because it is one of the most practical ones. The main
 215 concept of this algorithm is based on a model of the neuron that has two tasks. It aggregates signals
 216 (1) and then processes them by an activation function (2), which, in this research, is a sigmoid. The
 217 result of such single processing is a new signal z_j propagated to other neurons (Figure 3).



218
 219 Figure 3. Mathematical model of single neuron cell.

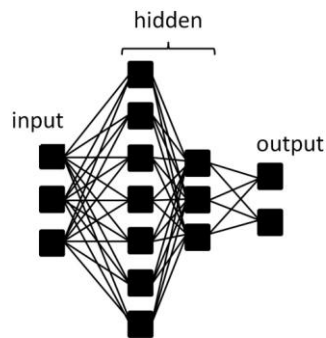
$$220 \quad a_j = \sum_i w_{ji} z_i \quad (1)$$

221
 222 a_j - aggregated signal, w_{ji} - weight that connects neuron i with j , z_i - signal (input).

$$223 \quad g(a_j) = \frac{1}{1 + e^{-\beta a_j}} \quad (2)$$

224
 225 $g(a_j)$ – sigmoidal function, β - parameter (steepness) of sigmoid curve.

226
 227 The structure of a neural network is formed by layers of neurons: input, hidden and output. In
 228 this research input neurons constitute a fluorescence spectrum and output neurons represent
 229 substances. Most computations are carried out in the hidden layers (no more than two layers were
 230 examined). The schematic representation of neuron layers is presented in Figure 4.



231
 232 Figure 4. Typical topology of an artificial neural network.

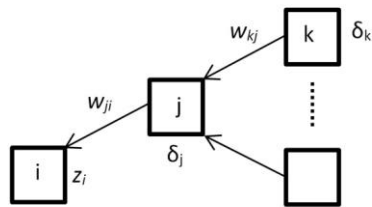
233
 234 The described algorithm constitutes the supervised learning method that requires training data

235 for a teaching process. This allows one to calculate an error between the target shown and the ANN
 236 response. Every problem is related to minimizing output error which is calculated as Mean Squared
 237 Error (3).

$$E = \frac{1}{2} \sum_{k=1}^c (y_k - t_k)^2 \quad (3)$$

238 E – Mean Squared Error, t_k - observed value (target), y_k - calculated response, k -output neuron, c –
 239 number of output neurons.

240 The gradient descent method is used to find a minimum of error function. Error is dependent on
 241 network weights Δw_{ji} which might be adjusted (4). In order to update weights correctly, firstly one
 242 needs to propagate error backwards by calculating partial derivatives δ_j (5) (Figure 5). All
 243 mathematical details are well described by C. M. Bishop (Bishop, 1995).



244
 245 Figure 5. Model of backward error propagation.

$$\Delta w_{ji}(t) = -\eta \delta_j z_i + m \Delta w_{ji}(t - 1) \quad (4)$$

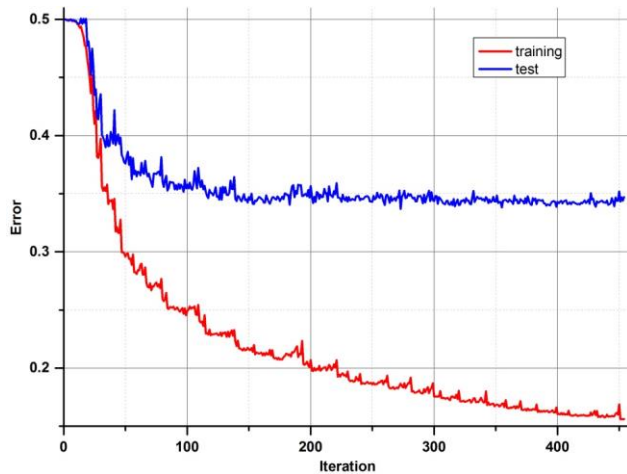
246 η - learning rate, m - momentum, t - iteration.

247

$$\frac{\delta E}{\delta w_{ji}} = \frac{\delta E}{\delta a_j} \frac{\delta a_j}{\delta w_{ji}} = \delta_j z_i \quad \delta_j = g'(a_j) \sum_k w_{kj} \delta_k \quad (5)$$

248 The learning rate factor determines the size of the steps while the momentum parameter
 249 enables the local minimum to be omitted by adding a fraction of the weight correction from the last
 250 step.

251 After the correction of all weights of the ANN, the output error is examined, and the procedure
 252 starts again unless an error level is low enough and there is no overfitting. All data are divided into
 253 three different sets: training, test and validation. For calculations during the learning process, only
 254 the first two are used. In order to determine whether it is time to stop the teaching process, one has
 255 to observe an error in the test set. There will be a moment when this error comes to be constant or
 256 starts increasing due to the overfitting of training data (Figure 6). The validation data set may be
 257 useful for comparing different models or just to verify the current model on a completely separate
 258 set of data.



259

260 Figure 6. Example of error minimizing during the training process.

261 **3.2.1.2. Implementation of ANN for BARDet**

262 There are statistical commercial software packages available that provide ANN modules as one
 263 of the methods to analyze the data. It is worthwhile noting that customized software was developed
 264 for this research. This approach helped us to understand ANNs in depth and led to the development
 265 of software that is not only responsible for data pre-processing and network training, but also
 266 (mainly) for solving a real time classification problem.

267 Ruske et al. in their studies (Ruske et al., 2017) compared various algorithms to analyze single
 268 particle data and noted that an ANN requires much more user input. However, we present a method
 269 to overcome this inconvenience by automating the process and implementing procedures which
 270 simplify and improve the analysis.

271 The main disadvantage of an ANN is the fact that it is a parametrized algorithm. How well it
 272 works depends strictly on a proper choice of the best possible factors, which may be different for
 273 each problem. There are two types of factors that influence the ANN outcome. The first one
 274 corresponds to the architecture of the ANN which comprises a number of layers, neurons and an
 275 activation function parameter. The second one determines the learning process: momentum and
 276 learning rate. The latter can be tuned during the learning process to make it much faster. The “bold
 277 driver” procedure was chosen for that purpose. It continuously increases the learning rate unless an
 278 error is higher from that before the change. If it is, the algorithm radically decreases the learning rate
 279 and obtains weights from the last step again. Teaching an ANN is a stochastic process initiated by
 280 using randomly chosen initial weights. It was found that the best procedure for this investigation
 281 would be to conduct all optimization processes that way. Therefore, the parameters of the ANN,
 282 responsible both for structure and learning process, are randomly selected until the desired result is
 283 reached. In fact, the calculations are carried out automatically and simultaneously for several models
 284 by means of multi core-oriented software. The benefits of this approach are time saving and high
 285 levels of efficiency and effectiveness in finding the best model. The latter is especially important,
 286 because the goal is to create a model that produces the best results, which doesn’t necessary mean

287 creating a more complicated network (more neurons or layers).

288 **3.2.2. Model evaluation**

289 The main goal of the analysis described in this paper is to find a solution to the bio-aerosol
290 classification problem. When a training process ends, a final model is created, a network, which has a
291 unique structure and a set of weights. One can create many of them and make a comparison only by
292 using the final error. It is not the best solution, because the goal is to distinguish patterns in data
293 consistently, not to produce a network with a minimal error. That is why there is a need to make a
294 final analysis of the results and evaluate the model in accordance with the best classification
295 performance.

296 The standard method for visualization of results is a confusion matrix which will be necessary for
297 Receiver Operating Characteristics (ROC) analysis (Fawcett, 2006). It simply shows what fraction of
298 population for each class is predicted correctly or not. Each element from the data set is assigned to
299 one of the following fits of the confusion matrix: True Positive (TP), True Negative (TN), False
300 Negative (FN) and False Positive (FP). If it belongs to TP and TN, it was classified correctly.

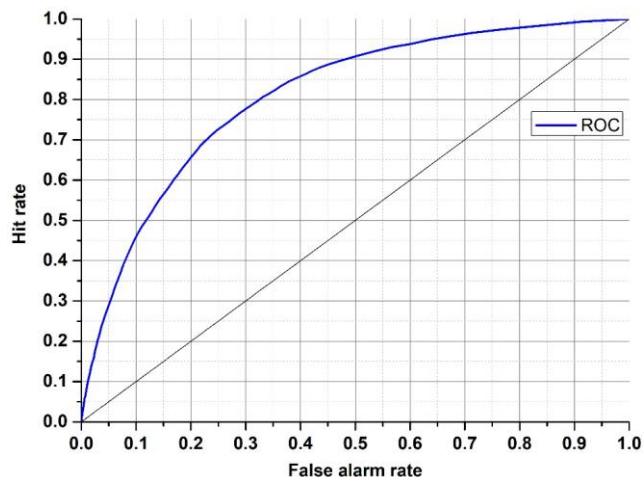
301 The ROC graphs are very simple but useful tools for discovering whether a classifier is worth
302 using or if it makes a random classification. It is based on two rates from the confusion matrix: hit
303 rate (6) and false alarm rate (7).

$$\begin{aligned} & \textit{hit rate (true positive rate)} \\ & = \frac{TP}{TP + FN} \end{aligned} \quad (6)$$

304

$$\begin{aligned} & \textit{false alarm rate (false positive rate)} \\ & = \frac{FP}{FP + TN} \end{aligned} \quad (7)$$

305 Each discrete classifier has a threshold level that assigns an element to a positive or negative
306 class. The points on the ROC graph (Figure 7) represent the classifier for many thresholds. The most
307 desirable curve will be obtained when the true positive rate is high, and the false positive rate is low
308 (convex line). The random classifier, in turn, has a hit rate equal to a false alarm rate despite
309 threshold variation (diagonal line). To identify an ROC analysis with one coefficient, the area under
310 the curve (AUC) may be used. The higher value of AUC results in better performance (0.5 means
311 random, 1 - excellent).



312

313 Figure 7. ROC graph with an example of classifier (blue).

314 The confusion matrix and ROC analysis described above were defined for two class problems
 315 (positive, negative). There is a straightforward way to expand it for multi-class problems. One needs
 316 to take a desired class versus all other classes. Then it will be possible to compare how good the
 317 classifier for specific classes within one model is.

318 **4. Results**

319 **4.2. ANN performance**

320 The first attempts were made to distinguish all substances using only one neural network model.
 321 The tests revealed that it is impossible due to the huge number of samples (48 aerosols) and only a
 322 few of them presented significantly different fluorescence spectra which allow accurate
 323 characterization. The remaining substances are then misclassified. Therefore, we decided to use a
 324 more practical approach to this problem, which would be to create several groups (considering
 325 information about aerosols), but we did not want to make any classes *a priori*. Although the ANN
 326 type demonstrated needs training, which requires a set of known classes, further tests showed that
 327 there is a possibility of finding similarities between substances through the analysis of confusion
 328 matrices. It was achieved after many trials of matching substances, which were not well separated,
 329 into new groups and checking if they are good enough on ROC graphs. Consequently, this procedure
 330 was also applied to those new groups.

331

332 All examples demonstrated below were calculated on the test data sets, not training data. In the
 333 first presented (Figure 8), which tries to classify all of the 48 substances (group 0), four aerosols
 334 reached a very high accuracy of separation (AUC>0,9). The best separation was achieved for
 335 fluorescent microspheres (FM). In this case 98.5% of all FM particles were correctly classified.
 336 Similarly, an efficient separation was achieved for riboflavin (RIB), Talc (NT) and [Lactobacillus](#)
 337 [bulgaricus](#) (LCB). The remaining aerosols were divided into 3 separate groups that gather the most
 338 similar substances (group 1-3) (Table 3). The subsequent groups up to 21 represent individual ANNs
 339 leading to the final classification of the aerosol. In practice separation is done not by one confusion
 340 matrix (ANN) but by all of them in sequence (22 ANNs combined in a decision tree). For example, if

341 an ANN classifies unknown substance into any of 22 groups it means that decision process is not
 342 ended but from that moment another ANN classifies this substance. However, each new ANN is
 343 trained using only a subsection of the data excluding the data from other groups.

344

345 Table 3. Exemplary confusion matrix of all aerosols classified by the first ANN.

346

		predicted						
		FM	RIB	NT	LCB	group 3	group 1	group 2
true	FM	98.5	0	0	0.3	0.1	0	1.1
	RIB	0.1	91	0.5	3.1	1.2	0.6	3.4
	NT	0	0.1	86.5	0	9.3	0.3	3.8
	LCB	1	1.6	0.6	72.7	3.9	10.7	9.5
	group 3	0	0.7	6.6	0.6	63.3	12	16.8
	group 1	0.2	1	1	7.9	12.5	61.6	15.8
	group 2	0.1	1.2	3.8	6.6	17.6	13.2	57.4

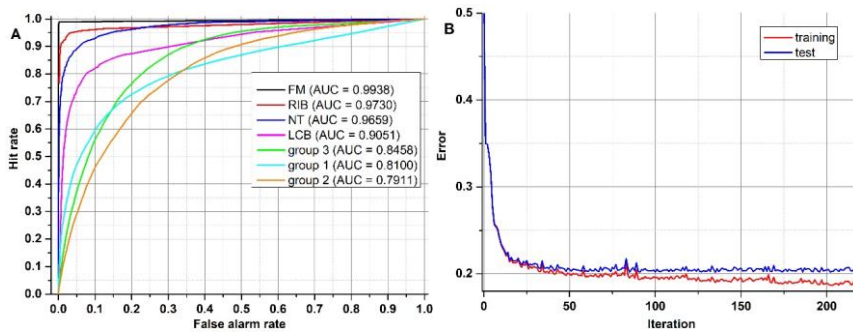
Formatted Table

Deleted: 7

Deleted: ib

Deleted: 7

Deleted: ib



347

348 Figure 8. (A) ROC and (B) error progress of ANN that classifies all samples.

349 Table 4 and Figure 9 show results achieved for two substances that have a very similar spectrum
 350 and the AUCs calculated are not much higher than in a random classifier. This example clearly shows
 351 why we are not always able to classify every single particle of aerosol with 100% accuracy. However,
 352 just a representative number (several dozen) of measured particles (a cloud) allows the proper
 353 prediction of aerosol types within a few seconds. This is easy to observe during real time detection,
 354 because counts allocated in a confusion matrix tend to reach a stable state quite quickly.

355

		predicted	
		BWF	CEL
true	BWF	54.8	45.2
	CEL	45.6	54.4

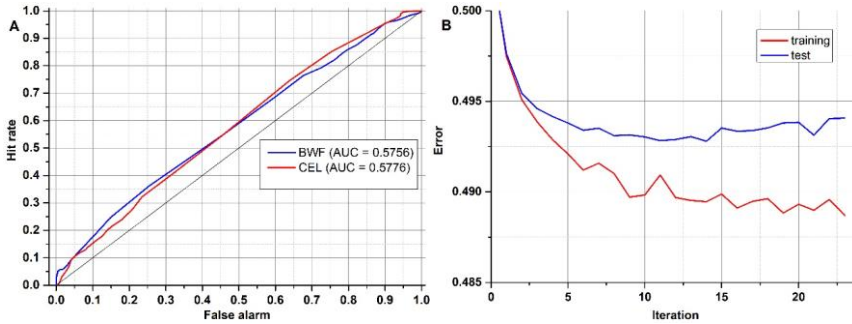
Formatted Table

Deleted: Cel

Formatted Table

Deleted: Cel

356 Table 4. Confusion matrix of two substances that have very similar spectra.

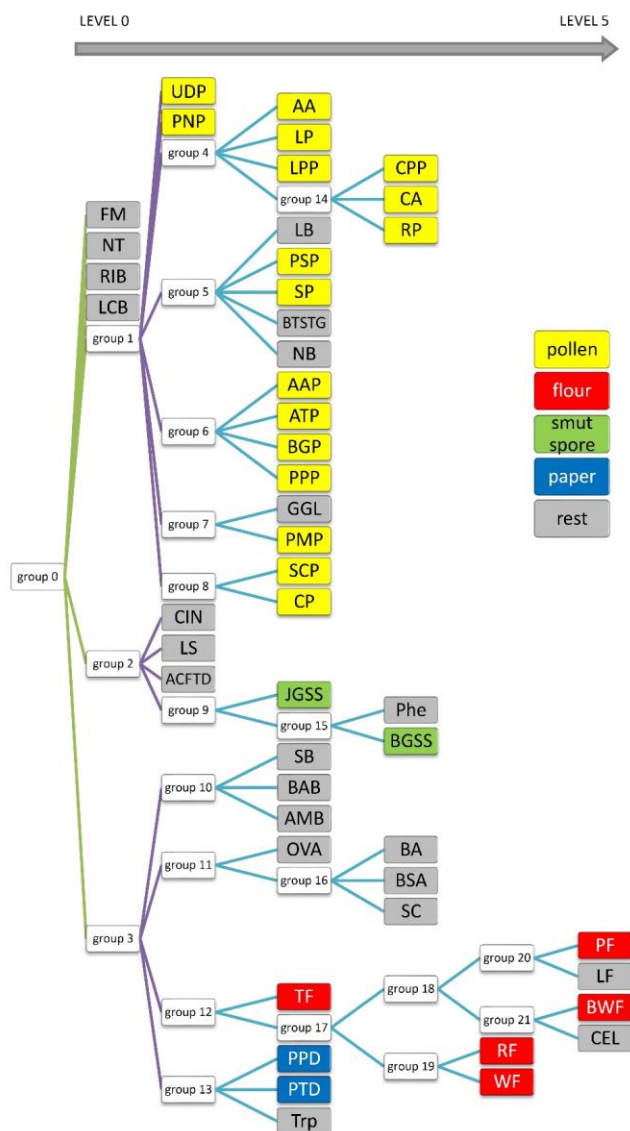


363
364 Figure 9. ROC (A) and error progress (B) of ANN which classify two very similar samples.

365
366 **4.3. Classification tree**

367 Finally, to achieve the best possible classification, a decision tree was created (Figure 10). It
 368 comprises not one, but 22 models. [The process of creating them is not replicable in terms of the](#)
 369 [exact factors used for ANN generation. However, this is not essential, because the decision tree is](#)
 370 [based on ANN results \(classification ability\), which should be possibly the highest. Therefore, the final](#)
 371 [result will be the same.](#) It is difficult to present confusion matrices and ROC graphs for all neural
 372 networks in this paper. Therefore, only the most interesting one has been discussed. Here, each node
 373 represents a network that classifies a group of aerosols. The aerosols on the left side of the diagram
 374 show the most distinct differences, thus they are easy to classify (Level 0). On the right side (Level 1-
 375 5), this task is much more demanding due to a similar spectrum and the separation is less probable in
 376 accordance with single particles, although it is still very useful from a practical point of view for
 377 aerosol cloud discrimination.

Deleted: be



379
380 Figure 10. The decision tree consists of 22 ANNs separating 48 substances.

381 At first glance one can see that FM and RIB are very well recognized, but that was expected
382 because these are standards of fluorescence. Surprisingly, NT and LCB aerosols were also separated
383 from the others (level 0 network). Further analysis of the tree structure identifies a correlation
384 between samples and their real categories. It is especially noticeable for pollens, which are allocated
385 to a separate branch of that tree, and all stems from group 1. Most of them were classified on the
386 third level. Interestingly all grass pollens (AAP, ATP, BGP, PPP) belong to the same group, 6. Similarly,

387 both *Lycopodium* pollens from different regions of the world show a close correlation, although *Abies*
388 *alba*, which is a tree, was classified in the same group. Flours, Spores and Papers are dispersed
389 between different levels, but particular groups belong to the same branch of the tree. However, some
390 of the samples are scattered on the whole tree area and do not correspond to any group.

391 It should be noted that the result is a system of 22 ANNs that work simultaneously. In
392 comparison to the training process, which is rather time consuming and has to be empirically
393 optimized, this cluster of learned ANNs delivers high performance. Input data is processed by a single
394 ANN in milliseconds. This performance makes the neural network a great tool as a splitting node in
395 the classification tree. Compared to our previous results, where Principal Component Analysis was
396 applied to analyze data from BARDet (Kaliszewski et al., 2016), the ANNs allowed much better
397 discrimination between various bio-aerosols.

398 5. Summary

399 In this paper the possibility of applying an Artificial Neural Network (ANN) for real time
400 classification of biological aerosols was investigated. The spectral characteristics of bio-aerosols were
401 collected using the BARDet instrument. The database consisted of 48 substances. Finally, 22 neural
402 networks were trained and combined into a decision tree. This allowed aerosols to be
403 characterized in real time. Tests revealed that only certain substances have such characteristic
404 fluorescence spectra that allow correct classification of almost each particle. However, in all other
405 cases the system was able to recognize a particular aerosol accurately with no mistake, but a
406 representative number of several dozens of particles in a cloud was necessary. Further
407 approximation was based on decision tree analysis where each node corresponded to a separate
408 learned ANN. The best sets of ANNs for each group of similar aerosols were discovered utilizing
409 confusion matrices and ROC analysis. Our intention was to make a complete system which detects
410 and classifies substances without creating groups *a priori*. This attitude helped us to create a
411 powerful analytical tool that works automatically, and the results of classification are immediately
412 available on the operator's screen.

413 This study proved that it is possible to create a tool for a highly effective analysis of bio-aerosols
414 using multiple ANNs combined into a decision tree. Our approach allowed us to automate and speed
415 up the analysis, which reduced time and the amount of computing power needed. In a future study
416 the database will be extended to obtain potentially a vast variety of samples including
417 atmospherically relevant bacteria and fungi. In the next step, the actual performance of the system
418 will be determined under real environmental conditions, [which will be most challenging due to the](#)
419 [presence of unknown fluorescent and non-fluorescent particles.](#)

420

421 Data availability

422 The experimental aerosol data can be provided upon request. The software for automatic data
423 analysis cannot be publicly provided at this moment since it is a subject of negotiations with a
424 company.

425

426 Acknowledgments

427 The work presented was supported by a grant from The National Centre of Research and
428 Development (Poland), within the project "Mobile laboratory for environmental sampling and
429 identification of biological threats" (O ROB 0031 01/ID/31/1).

430

431 **References**

- 432 Agranovski, V., Ristovski, Z., Hargreaves, M., Blackall, P. J. and Morawska, L.: Performance
433 evaluation of the UVAPS: Influence of physiological age of airborne bacteria and bacterial
434 stress, *J. Aerosol Sci.*, 34(12), 1711–1727, doi:10.1016/S0021-8502(03)00191-5, 2003.
- 435 Antowiak, M. and Asińska-macukow, K. C. H. a: Fingerprint identification by using artificial
436 neural network with optical wavelet preprocessing, , 11(4), 327–337, 2003.
- 437 Purnomo, H. D., Hartomo, K. D. and Prasetyo, S. Y. J.: Artificial Neural Network for Monthly
438 Rainfall Rate Prediction , *IOP Conf. Ser. Mater. Sci. Eng.*, 180(1), 12057, doi:10.1088/1742-
439 6596/755/1/011001, 2017.
- 440 Bhangar, S., Huffman, J. A. and Nazaroff, W. W.: Size-resolved fluorescent biological aerosol
441 particle concentrations and occupant emissions in a university classroom, *Indoor Air*, 24(6),
442 604–617, doi:10.1111/ina.12111, 2014.
- 443 Bishop, C. M.: Neural networks for pattern recognition, Oxford University Press, Inc., New
444 York, NY, USA., 1995.
- 445 Blais-Lecours, P., Perrott, P. and Duchaine, C.: Non-culturable bioaerosols in indoor settings:
446 Impact on health and molecular approaches for detection, *Atmos. Environ.*, 110, 45–53,
447 doi:10.1016/j.atmosenv.2015.03.039, 2015.
- 448 Borecki, M., Korwin-Pawłowski, M. L. and Beblowska, M.: A method of examination of liquids
449 by neural network analysis of reflectometric and transmission time domain data from optical
450 capillaries and fibers, in *IEEE Sensors Journal*, vol. 8, pp. 1208–1214., 2008.
- 451 Choi, K., Ha, Y., Lee, H. K. and Lee, J.: Development of a biological aerosol detector using
452 laser-induced fluorescence and a particle collection system, *Instrum. Sci. Technol.*, 42(2),
453 200–214, doi:10.1080/10739149.2013.855639, 2014.
- 454 Crawford, I., Ruske, S., Topping, D. O. and Gallagher, M. W.: Evaluation of hierarchical
455 agglomerative cluster analysis methods for discrimination of primary biological aerosol,
456 *Atmos. Meas. Tech.*, 8(11), 4979–4991, doi:10.5194/amt-8-4979-2015, 2015.
- 457 Davidson, C. I., Phalen, R. F. and Solomon, P. A.: Airborne particulate matter and human
458 health: A review, *Aerosol Sci. Technol.*, 39(8), 737–749, doi:10.1080/02786820500191348,
459 2005.
- 460 Deguillaume, L., Leriche, M., Amato, P., Ariya, P. a., Delort, A. M., Pöschl, U., Chaumerliac, N.,
461 Bauer, H., Flossmann, a. I. and Morris, C. E.: Microbiology and atmospheric processes:
462 chemical interactions of Primary Biological Aerosols, *Biogeosciences Discuss.*, 5(1), 841–870,
463 doi:10.5194/bgd-5-841-2008, 2008.
- 464 Fawcett, T.: An introduction to ROC analysis. *Pattern Recognition Letters*, *Pattern Recognit.*
465 *Lett.*, 27(8), 861–874, doi:https://doi.org/10.1016/j.patrec.2005.10.010, 2006.
- 466 Fennelly, M. J., Sewell, G., Prentice, M. B., O'Connor, D. J. and Sodeau, J. R.: Review: The use
467 of real-time fluorescence instrumentation to monitor ambient primary biological aerosol
468 particles (PBAP), *Atmosphere (Basel)*, 9(1), doi:10.3390/atmos9010001, 2017.
- 469 Feugnet, G., Lallier, E., Grisard, A., McIntosh, L., Hellström, J. E., Jelger, P., Laurell, F., Albano,
470 C., Kaliszewski, M., Włodarski, M., Mlynczak, J., Kwasny, M., Zawadzki, Z., Mierczyk, Z.,
471 Kopczynski, K., Rostedt, A., Putkiranta, M., Marjamäki, M., Keskinen, J., Enroth, J., Janka, K.,

472 Reinivaara, R., Holma, L., Humpi, T., Battistelli, E., Iliakis, E. and Gerolimos, G.: Improved
473 laser-induced fluorescence method for bio-attack early warning detection system, in
474 Proceedings of SPIE - The International Society for Optical Engineering, vol. 7116, p. 71160C,
475 Thales Research and Technology, France., 2008.

476 Fröhlich-Nowoisky, J., Kampf, C. J., Weber, B., Huffman, J. A., Pöhlker, C., Andreae, M. O.,
477 Lang-Yona, N., Burrows, S. M., Gunthe, S. S., Elbert, W., Su, H., Hoor, P., Thines, E.,
478 Hoffmann, T., Després, V. R. and Pöschl, U.: Bioaerosols in the Earth system: Climate, health,
479 and ecosystem interactions, *Atmos. Res.*, 182, 346–376,
480 doi:10.1016/j.atmosres.2016.07.018, 2016.

481 Fuzzi, S., Baltensperger, U., Carslaw, K., Decesari, S., Denier Van Der Gon, H., Facchini, M. C.,
482 Fowler, D., Koren, I., Langford, B., Lohmann, U., Nemitz, E., Pandis, S., Riipinen, I., Rudich, Y.,
483 Schaap, M., Slowik, J. G., Spracklen, D. V., Vignati, E., Wild, M., Williams, M. and Gilardoni, S.:
484 Particulate matter, air quality and climate: Lessons learned and future needs, *Atmos. Chem.*
485 *Phys.*, 15(14), 8217–8299, doi:10.5194/acp-15-8217-2015, 2015.

486 Gabey, A. M., Gallagher, M. W., Whitehead, J., Dorsey, J. R., Kaye, P. H. and Stanley, W. R.:
487 Measurements and comparison of primary biological aerosol above and below a tropical
488 forest canopy using a dual channel fluorescence spectrometer, *Atmos. Chem. Phys.*, 10(10),
489 4453–4466, doi:10.5194/acp-10-4453-2010, 2010.

490 Gabey, A. M., Stanley, W. R., Gallagher, M. W. and Kaye, P. H.: The fluorescence properties
491 of aerosol larger than 0.8 μ in urban and tropical rainforest locations, *Atmos. Chem. Phys.*,
492 11(11), 5491–5504, doi:10.5194/acp-11-5491-2011, 2011.

493 Górný, R. L.: Filamentous microorganisms and their fragments in indoor air - A review, *Ann.*
494 *Agric. Environ. Med.*, 11(2), 185–197, doi:10.1007/BF02677055, 2004.

495 Hernandez, M., Perring, A. E., McCabe, K., Kok, G., Granger, G. and Baumgardner, D.:
496 Chamber catalogues of optical and fluorescent signatures distinguish bioaerosol classes,
497 *Atmos. Meas. Tech.*, 9(7), 3283–3292, doi:10.5194/amt-9-3283-2016, 2016.

498 Hill, S. C., Pinnick, R. G., Niles, S., Pan, Y.-L., Holler, S., Chang, R. K., Bottinger, J., Chen, B. T.,
499 Orr, C.-S. and Feather, G.: Realtime Measurement of Fluorescence Spectra from Single
500 Airborne Biological Particles, *F. Anal. Chem. Technol.*, 3(4–5), 221–239,
501 doi:10.1002/(SICI)1520-6521(1999)3:4/5<221::AID-FACT2>3.3.CO;2-Z, 1999.

502 Huffman, J. A., Treutlein, B. and Pöschl, U.: Fluorescent biological aerosol particle
503 concentrations and size distributions measured with an Ultraviolet Aerodynamic Particle
504 Sizer (UV-APS) in Central Europe, *Atmos. Chem. Phys.*, 10(7), 3215–3233, doi:10.5194/acp-
505 10-3215-2010, 2010.

506 Kaliszewski, M., Trafny, E. A., Lewandowski, R., Włodarski, M., Bombalska, A., Kopczyński, K.,
507 Antos-Bielska, M., Szpakowska, M., Młyńczak, J., Mularczyk-Oliwa, M. and Kwaśny, M.: A
508 new approach to UVAPS data analysis towards detection of biological aerosol, *J. Aerosol Sci.*,
509 58, 148–157, doi:10.1016/j.jaerosci.2013.01.007, 2013.

510 Kaliszewski, M., Włodarski, M., Młyńczak, J., Leśkiewicz, M., Bombalska, A., Mularczyk-Oliwa,
511 M., Kwaśny, M., Buliński, D. and Kopczyński, K.: A new real-time bio-aerosol fluorescence
512 detector based on semiconductor CW excitation UV laser, *J. Aerosol Sci.*, 100, 14–25,
513 doi:10.1016/j.jaerosci.2016.05.004, 2016.

514 Kohlus, R. and Bottlinger, M.: Particle Shape Analysis as an example of knowledge extraction

515 by neural nets, Part. Part. Syst. Charact., 10(5), 275–278, doi:10.1002/ppsc.19930100511,
516 1993.

517 Lakowicz, J. R.: Principles of fluorescence spectroscopy, Second., Kluwer Academic/Plenum
518 Publishers., 2006.

519 Leśkiewicz, M., Kaliszewski, M., Mierczyk, Z. and Włodarski, M.: Comparison of Principal
520 Component Analysis and Linear Discriminant Analysis applied to classification of excitation-
521 emission matrices of the selected biological material, Biul. Wojsk. Akad. Tech., 65(1), 15–31,
522 doi:10.5604/12345865.1197960, 2016.

523 Lim, D. V., Simpson, J. M., Kearns, E. A. and Kramer, M. F.: Current and developing
524 technologies for monitoring agents of bioterrorism and biowarfare, Clin. Microbiol. Rev.,
525 18(4), 583–607, doi:10.1128/CMR.18.4.583-607.2005, 2005.

526 Mauderly, J. L. and Chow, J. C.: Health effects of organic aerosols, Inhal. Toxicol., 20(3), 257–
527 288, doi:10.1080/08958370701866008, 2008.

528 Miaskiewicz-Peska, E. and Lebkowska, M.: Comparison of aerosol and bioaerosol collection
529 on air filters, Aerobiologia (Bologna), 28(2), 185–193, doi:10.1007/s10453-011-9223-1,
530 2012.

531 Michaels, R. A.: Environmental Moisture, Molds, and Asthma—Emerging Fungal Risks in the
532 Context of Climate Change, Environ. Claims J., 29(3), 171–193,
533 doi:10.1080/10406026.2017.1345521, 2017.

534 Pan, Y. Le, Hill, S. C., Pinnick, R. G., House, J. M., Flagan, R. C. and Chang, R. K.: Dual-
535 excitation-wavelength fluorescence spectra and elastic scattering for differentiation of single
536 airborne pollen and fungal particles, Atmos. Environ., 45(8), 1555–1563,
537 doi:10.1016/j.atmosenv.2010.12.042, 2011.

538 Pan, Y. Le, Huang, H. and Chang, R. K.: Clustered and integrated fluorescence spectra from
539 single atmospheric aerosol particles excited by a 263- and 351-nm laser at New Haven, CT,
540 and Adelphi, MD, J. Quant. Spectrosc. Radiat. Transf., 113(17), 2213–2221,
541 doi:10.1016/j.jqsrt.2012.07.028, 2012.

542 Pinnick, R. G., Hill, S. C., Pan, Y. Le and Chang, R. K.: Fluorescence spectra of atmospheric
543 aerosol at Adelphi, Maryland, USA: Measurement and classification of single particles
544 containing organic carbon, Atmos. Environ., 38(11), 1657–1672,
545 doi:10.1016/j.atmosenv.2003.11.017, 2004.

546 Pöhlker, C., Huffman, J. A. and Pöschl, U.: Autofluorescence of atmospheric bioaerosols:
547 Spectral fingerprints and taxonomic trends of pollen, Atmos. Meas. Tech., 6(12), 3369–3392,
548 doi:10.5194/amt-6-3369-2013, 2013.

549 Pope, C. A. and Dockery, D. W.: Health effects of fine particulate air pollution: Lines that
550 connect, J. Air Waste Manag. Assoc., 56(6), 709–742, doi:10.1080/10473289.2006.10464485,
551 2006.

552 Pósfai, M. and Buseck, P. R.: Nature and Climate Effects of Individual Tropospheric Aerosol
553 Particles, Annu. Rev. Earth Planet. Sci., 38(1), 17–43,
554 doi:10.1146/annurev.earth.031208.100032, 2010.

555 Ruske, S., Topping, D. O., Foot, V. E., Kaye, P. H., Stanley, W. R., Crawford, I., Morse, A. P. and
556 Gallagher, M. W.: Evaluation of machine learning algorithms for classification of primary

557 biological aerosol using a new UV-LIF spectrometer, *Atmos. Meas. Tech.*, 10(2), 695–708,
558 doi:10.5194/amt-10-695-2017, 2017.

559 Savage, N. J., Krentz, C. E., Könnemann, T., Han, T. T., Mainelis, G., Pöhlker, C. and Alex
560 Huffman, J.: Systematic characterization and fluorescence threshold strategies for the
561 wideband integrated bioaerosol sensor (WIBS) using size-resolved biological and interfering
562 particles, *Atmos. Meas. Tech.*, 10(11), 4279–4302, doi:10.5194/amt-10-4279-2017, 2017.

563 Shiraiwa, M., Selzle, K. and Pöschl, U.: Hazardous components and health effects of
564 atmospheric aerosol particles: Reactive oxygen species, soot, polycyclic aromatic compounds
565 and allergenic proteins, *Free Radic. Res.*, 46(8), 927–939,
566 doi:10.3109/10715762.2012.663084, 2012.

567 Taketani, F., Kanaya, Y., Nakamura, T., Koizumi, K., Moteki, N. and Takegawa, N.:
568 Measurement of fluorescence spectra from atmospheric single submicron particle using
569 laser-induced fluorescence technique, *J. Aerosol Sci.*, 58, 1–8,
570 doi:10.1016/j.jaerosci.2012.12.002, 2013.

571 Trafny, E. A., Lewandowski, R., Stępińska, M. and Kaliszewski, M.: Biological threat detection
572 in the air and on the surface: How to define the risk, *Arch. Immunol. Ther. Exp. (Warsz.)*,
573 62(4), 253–261, doi:10.1007/s00005-014-0296-8, 2014.

574 Uk Lee, B., Jung, J. H., Yun, S. H., Hwang, G. B. and Bae, G. N.: Application of UVAPS to real-
575 time detection of inactivation of fungal bioaerosols due to thermal energy, *J. Aerosol Sci.*,
576 41(7), 694–701, doi:10.1016/j.jaerosci.2010.04.003, 2010.

Formatted: Space Before: 0 pt